Elsevier Editorial System(tm) for International Journal of Solids and Structures

Manuscript Draft

Manuscript Number: IJSS-D-06-00776R1

Title: Controlling parameter of the stress intensity factors for a planar interfacial crack in three-dimensional bimaterials

Article Type: Research Paper

Keywords: Elasticity, Stress intensity factor, Body force method, Interface crack, Singular integral equation.

Corresponding Author: Dr N.-A. Noda,

Corresponding Author's Institution: Kyushu Institute of Technology

First Author: N.-A. Noda

Order of Authors: N.-A. Noda; chunhui Xu

Abstract: Numerical solutions of singular integral equations are discussed in the analysis of a planar rectangular interfacial crack in three-dimensional bimaterials. The problem is formulated as a system of singular integral equations on the basis of the body force method. In the numerical analysis, unknown body force densities are approximated by the products of the fundamental density functions and power series, where the fundamental density functions are chosen to express singular behavior along the crack front of the interface crack exactly. The calculation shows that the present method gives smooth variations of stress intensity factor along the crack front for various aspect ratios. The present method gives rapidly converging numerical results and highly satisfied boundary conditions throughout the crack boundary. The stress intensity factors are given with varying the material combination and aspect ratio of the crack. It is found that the stress intensity factors and are determined by the bimaterial constant alone, independent of elastic modulus ratio and Poisson's ratio.

Controlling parameter of the stress intensity factors for a planar interfacial crack in three-dimensional bimaterials

Nao-Aki NODA [1] and Chunhui Xu[2]

1 Dept. of Mechanical Engineering, Kyushu Institute of Technology, 1-1, Sensui-cho, Tobata, Kitakyushu, 804-8550, JAPAN

2 College of Science, China Agricultural University,

Beijing 100083, P.R.CHINA

(Current address: Mechanical Engineering Department, Kyushu Institute of Technology,1-1, Sensui-cho, Tobata, Kitakyushu 804-8550, JAPAN)

Abstract: Numerical solutions of singular integral equations are discussed in the analysis of a planar rectangular interfacial crack in three-dimensional bimaterials. The problem is formulated as a system of singular integral equations on the basis of the body force method. In the numerical analysis, unknown body force densities are approximated by the products of the fundamental density functions and power series, where the fundamental density functions are chosen to express singular behavior along the crack front of the interface crack exactly. The calculation shows that the present method gives smooth variations of stress intensity factor along the crack front

for various aspect ratios. The present method gives rapidly converging numerical results and highly satisfied boundary conditions throughout the crack boundary. The stress intensity factors are given with varying the material combination and aspect ratio of the crack. It is found that the stress intensity factors K_I and K_{II} are determined by the bimaterial constant ε alone, independent of elastic modulus ratio and Poisson's ratio.

Key words: Elasticity, Stress intensity factor, Body force method, Interface crack, Singular integral equation.

Notations

$2a \times 2b$ Dimensions of rectangular crack

μ_1, μ_2 Shear modulus for space 1 and space 2

ν_1, ν_2 Poisson’s ratio for space 1 and space 2

(x, y, z) Rectangular coordinate

(ξ, η, ζ) Rectangular coordinate (x, y, z) where the body force is applied

ε Bimaterial constant $= \frac{1}{2\pi} \ln\left(\frac{\mu_2 \kappa_1 + \mu_1}{\mu_1 \kappa_2 + \mu_2} \right)$

$w_z(\xi, \eta), w_y(\xi, \eta), w_x(\xi, \eta)$ Fundamental body force densities to express the stress fields due to a rectangular crack in an infinite body under uniform tension σ_z^∞

$f_{zz}(\xi,\eta), f_{yz}(\xi,\eta), f_{zx}(\xi,\eta)$ Unknown body force densities, which are equivalent to the displacement discontinuities

$\alpha_i, \beta_i, \gamma_i$ Unknown coefficient

(u_x, u_y, u_z) Displacement in (x, y, z) direction

$\Delta u_x(x, y)$ Crack opening displacement $= u_x(x, y, +0) - u_x(x, y, -0)$

$\Delta u_y(x, y)$ Crack opening displacement $= u_y(x, y, +0) - u_y(x, y, -0)$

$\Delta u_z(x, y)$ Crack opening displacement $= u_z(x, y, +0) - u_z(x, y, -0)$

K_I, K_{II}, K_{III} Stress intensity factors

F_I, F_{II}, F_{III} Dimensionless stress intensity factors normalized by $\sigma_z^{\infty}\sqrt{\pi b}$

1. Introduction

In recent years, composite materials and adhesive or bonded joints are being used in wide range of engineering field. With the rapidly increasing the use of composite materials and adhesive, much attention has been paid to the interface because the fracture is usually originated from the interfacial region. It is desirable to design and manufacture composite structures whose fracture behavior is known at their interface. Although a lot of studies have been made for interface cracks problems (Comninou, 1977; England, 1965; Erdogan, 1963, 1965; England and Gupta, 1975; Noda and Oda, 1997; Rice and Sih, 1965; Salganik, 1963; Tucker, 1974; Willis, 1971; Willis, 1972), most of these works are on

two-dimensional cases. The numerical solutions were discussed in the analysis of a penny-shaped crack between two dissimilar materials (England, 1965; Kassir and Bregman, 1972; Lowengrub, and Senddon, 1974; Mossakovski and Rybka, 1964; Shibuya-Koizumi-Iwamoto, 1989). Due to the mathematical difficulties, few analytical methods are available for three-dimensional interface cracks under general material combinations and general aspect ratio. Considering this situation, Noda–Kagita-Chen (2003) evaluated the stress intensity factors of an axi-symmetric interface cracks under torsion and tension by the body force method for general material combinations.

The body force method was originally proposed by Nisitani (1967) as a new method for solving stress concentration problems. In solving crack problems, the body force method uses the stress fields due to a pair of point forces or displacement discontinuities (Nisitani-Murakami, 1974). In those analyses, the problems are formulated as a system of singular integral equations. Then, accurate numerical solutions were investigated in the previous studies (Noda and Oda, 1992; Noda and Matsuo, 1998). For a semi-elliptical surface crack, Noda and Miyoshi (1996) studied the variation of stress intensity factor and crack opening displacement using a hypersingular integral equation, where the unknown body force density was approximated by the products of fundamental density

function and polynomial. Here, the fundamental density was chosen to express the stress field due to an elliptical crack in an infinite body exactly. This numerical method was applied to investigate the stress intensity factors of a 3D rectangular crack using the body force method (Wang and Noda, 2001).

For planar interface crack problems, hypersingular intergro-differential equations were indicated as a general expression (Chen-Noda-Tang, 1999). However, solving the equations is extremely difficult because of the oscillation singularity and overlapping of crack surfaces, both of which are peculiar to interface cracks. In this paper, numerical solutions will be considered for a planar rectangular interface crack on the basis of the equations. Here, the fundamental density functions will be chosen to express singular behavior along the crack front of the interface crack exactly. Then, it will be shown that the smooth variations of stress intensity factor along the crack front are highly satisfactory boundary conditions throughout the crack surface. The influence of the dimension of the interfacial crack and of the ratio of the elastic parameter will be shown completely and exhaustively.

2 Singular integral equations for a planar interfacial crack

Consider two dissimilar elastic half-spaces bonded together along

the x–y plane (see Fig.1) with a fixed rectangular Cartesian

Fig.1

coordinate system x_i $(i = x, y, z)$. Suppose that the upper half-space is occupied by an elastic medium with constants (μ_1, ν_1), and the lower half-space by an elastic medium with constants (μ_2, ν_2). Here, μ_1, μ_2 are shear modulus for space 1 and space 2, and ν_1, ν_2 are Poisson's ratio for space 1 and space 2. The crack is assumed to be located at the bimaterial interface.

Hypersingular intergro-differential equations for three dimensional cracks on a bimateral interface in Fig.1 were derived by Chen–Noda-Tang (1999) and expressed as shown in Eq.(1).

$$\mu_1(\Lambda_2-\Lambda_1)\frac{\partial \Delta u_z(x,y)}{\partial x}+\mu_1\frac{(2\Lambda-\Lambda_1-\Lambda_2)}{2\pi}\int_s\frac{1}{r^3}\Delta u_x(\xi,\eta)dS(\xi,\eta)$$
$$+3\mu_1\frac{(\Lambda_1+\Lambda_2-\Lambda)}{2\pi}\left\{\int_s\frac{(x-\xi)^2}{r^5}\Delta u_x(\xi,\eta)dS(\xi,\eta)+\int_s\frac{(x-\xi)(y-\eta)}{r^5}\Delta u_y(\xi,\eta)dS(\xi,\eta)\right\}=0 \quad (1a)$$

$$\mu_1(\Lambda_2-\Lambda_1)\frac{\partial \Delta u_z(x,y)}{\partial y}+\mu_1\frac{(2\Lambda-\Lambda_1-\Lambda_2)}{2\pi}\int_s\frac{1}{r^3}\Delta u_y(\xi,\eta)dS(\xi,\eta)$$
$$+3\mu_1\frac{(\Lambda_1+\Lambda_2-\Lambda)}{2\pi}\left\{\int_s\frac{(x-\xi)(y-\eta)}{r^5}\Delta u_x(\xi,\eta)dS(\xi,\eta)+\int_s\frac{(y-\eta)^2}{r^5}\Delta u_y(\xi,\eta)dS(\xi,\eta)\right\}=0 \quad (1b)$$

$$\mu_1(\Lambda_1-\Lambda_2)\left(\frac{\partial \Delta u_x(x,y)}{\partial x}+\frac{\partial \Delta u_y(x,y)}{\partial y}\right)+\mu_1\frac{(\Lambda_1+\Lambda_2)}{2\pi}\int_s \frac{1}{r^3}\Delta u_z(\xi,\eta)dS(\xi,\eta)=-p_z(x,y) \qquad (1c)$$

$$(x,y)\in S,$$

$$\Lambda=\frac{\mu_2}{\mu_1+\mu_2},\ \Lambda_1=\frac{\mu_2}{\mu_1+\kappa_1\mu_2},\ \Lambda_2=\frac{\mu_2}{\mu_2+\kappa_2\mu_1}, \qquad (1d)$$
$$\kappa_1=3-4\nu_1,\ \kappa_2=3-4\nu_2,\ r^2=(x-\xi)^2+(y-\eta)^2$$

$$\begin{aligned}
\Delta u_x(x,y)&=u_x(x,y,0^+)-u_x(x,y,0^-)=\sum_{l=1}^{2}\frac{1}{\mu_l}f_{zx}(x,y),\\
\Delta u_y(x,y)&=u_y(x,y,0^+)-u_y(x,y,0^-)=\sum_{l=1}^{2}\frac{1}{\mu_l}f_{yz}(x,y), \qquad (1e)\\
\Delta u_z(x,y)&=u_z(x,y,0^+)-u_z(x,y,0^-)=\sum_{l=1}^{2}\frac{\kappa_l-1}{\mu_l(\kappa_l+1)}f_{zz}(x,y).
\end{aligned}$$

In Eq.(1), unknown functions are crack opening displacements, in other words, displacement discontinuities $\Delta u_x, \Delta u_y, \Delta u_z$ defined in Eq.(1e), which are equivalent to the body force densities $f_{zx}(x,y)$, $f_{yz}(x,y)$, $f_{zz}(x,y)$ as shown in Eq.(1e). Here, (ξ,η,ζ) is a rectangular coordinate (x,y,z) where the displacement discontinuities are distributed, and p_x, p_y, p_z are the stresses τ_{zx}^{∞}, τ_{yz}^{∞}, σ_z^{∞} at infinity. As shown in Fig.1 (b), we can put $p_x=0$, $p_y=0$. Since the integral has a hypersingularity of the form r^{-3} when $x=\xi$ and $y=\eta$, the integration should be interpreted in a sense of a finite part integral in the region *S* (Hadamard, 1923).

3 Numerical solutions of the singular integral equations

Consider a rectangular interface crack under tension at infinity. In the numerical solution, it is necessary to express the oscillation singular stress, which is specific to the crack tip of interface cracks. For two-dimensional crack problems (see Fig.2), crack

Fig.2

opening displacement can be expressed in the following equations (Rice and Sih, 1965).

For Fig.2 (a): $$\Delta u_z + i\Delta u_x = \sum_{l=1}^{2}\left\{\frac{\kappa_l - 1}{\mu_l(1+\kappa_l)} w_z(\xi) + i\frac{1}{\mu_l} w_x(\xi)\right\} \times [\sigma_0 + i\tau_0]$$

$$= \sum_{l=1}^{2}\frac{1+\kappa_l}{4\mu_l \cosh \pi\varepsilon}\sqrt{a^2-\xi^2}\left(\frac{a-\xi}{a+\xi}\right)^{i\varepsilon} \times [\sigma_0 + i\tau_0], \quad (2a)$$

For Fig.2 (b): $$\Delta u_y = \sum_{l=1}^{2}\frac{1}{\mu_l} w_y(\xi)\tau_0 = \sum_{l=1}^{2}\frac{1}{\mu_l}\frac{1+\kappa_l}{4}\sqrt{a^2-\xi^2}\,\tau_0 \quad (2b)$$

$$\varepsilon = \frac{1}{2\pi}\ln\left(\frac{\mu_2\kappa_1 + \mu_1}{\mu_1\kappa_2 + \mu_2}\right) \quad (3)$$

$$\kappa_l = \begin{cases} \dfrac{3-\nu_l}{1+\nu_l} & \text{plane stress} \\ 3-4\nu_l & \text{plane strain} \end{cases} \quad (4)$$

Here, σ_0 , τ_0 are the stresses at infinity, and $w_1(\xi)$ and $w_2(\xi)$ are called fundamental density functions, which express stress fields due to a single 2D interface crack exactly (Nisitani-Saimoto-Noguchi,

1993).

In the present analysis, the fundamental densities and polynomials have been used to approximate the unknown functions as a continuous function. First, we put

$$\begin{aligned}\Delta u_x(\xi,\eta) &= w_x(\xi,\eta)F_x(\xi,\eta),\\ \Delta u_y(\xi,\eta) &= w_y(\xi,\eta)F_y(\xi,\eta),\\ \Delta u_z(\xi,\eta) &= w_z(\xi,\eta)F_z(\xi,\eta).\end{aligned} \tag{5}$$

Considering Eq.(2), for the three dimensional interface crack problem, the fundamental density function are expressed as the follows.

$$\left.\begin{aligned} w_x(\xi,\eta) &= \sum_{l=1}^{2}\frac{1+k_l}{4\mu_l\cosh\pi\varepsilon}\sqrt{a^2-\xi^2}\sqrt{b^2-\eta^2}\sin\left(\varepsilon\ln\left(\frac{a-\xi}{a+\xi}\right)\right)\\ w_y(\xi,\eta) &= \sum_{l=1}^{2}\frac{1+k_l}{4\mu_l\cosh\pi\varepsilon}\sqrt{a^2-\xi^2}\sqrt{b^2-\eta^2}\sin\left(\varepsilon\ln\left(\frac{b-\eta}{b+\eta}\right)\right)\\ w_z(\xi,\eta) &= \sum_{l=1}^{2}\frac{1+k_l}{4\mu_l\cosh\pi\varepsilon}\sqrt{a^2-\xi^2}\sqrt{b^2-\eta^2}\cos\left(\varepsilon\ln\left(\frac{a-\xi}{a+\xi}\right)\right)\cos\left(\varepsilon\ln\left(\frac{b-\eta}{b+\eta}\right)\right)\end{aligned}\right\} \tag{6}$$

The fundamental densities (6) lead to expressing the oscillation stress singularity and overlapping of crack surfaces along the crack front exactly. To satisfy the boundary conditions for the rectangle region of the interface crack, the following expressions may be applied, where the unknowns are coefficients of the polynomials $\alpha_i, \beta_i, \gamma_i$.

$$F_x(\xi,\eta)=\alpha_0+\alpha_1\eta+\cdots+\alpha_{n-1}\eta^{(n-1)}+\alpha_n\eta^n+\alpha_{n+1}\xi+\alpha_{n+2}\xi\eta+\cdots+\alpha_{2n}\xi\eta^n+\cdots$$
$$+\alpha_{l-n-1}\xi^m+\alpha_{l-n}\xi^m\eta+\cdots+\alpha_{l-1}\xi^m\eta^n=\sum_{i=0}^{l-1}\alpha_i G_i(\xi,\eta),$$

$$F_y(\xi,\eta)=\beta_0+\beta_1\eta+\cdots+\beta_{n-1}\eta^{(n-1)}+\beta_n\eta^n+\beta_{n+1}\xi+\beta_{n+2}\xi\eta+\cdots+\beta_{2n}\xi\eta^n+\cdots$$
$$+\beta_{l-n-1}\xi^m+\beta_{l-n}\xi^m\eta+\cdots+\beta_{l-1}\xi^m\eta^n=\sum_{i=0}^{l-1}\beta_i G_i(\xi,\eta),$$

$$F_z(\xi,\eta)=\gamma_0+\gamma_1\eta+\cdots+\gamma_{n-1}\eta^{(n-1)}+\gamma_n\eta^n+\gamma_{n+1}\xi+\gamma_{n+2}\xi\eta+\cdots+\gamma_{2n}\xi\eta^n+\cdots$$
$$+\gamma_{l-n-1}\xi^m+\gamma_{l-n}\xi^m\eta+\cdots+\gamma_{l-1}\xi^m\eta^n=\sum_{i=0}^{l-1}\gamma_i G_i(\xi,\eta), \qquad (7)$$

$$l=(m+1)(n+1),$$

$$G_0(\xi,\eta)=1,\ G_1(\xi,\eta)=\eta,\ \cdots,G_{n+1}(\xi,\eta)=\xi,\ \cdots,G_{l-1}(\xi,\eta)=\xi^m\eta^n.$$

By substituting Eqs(5),(6),(7)into Eq.(1), we obtain the following system of algebraic equations for the determination of coefficients $\alpha_i,\beta_i,\gamma_i$, which can be determined by selecting a set of collocation points(Noda-Kagita-Chen,2003; Noda and Miyoshi,1996).

$$\left.\begin{aligned}
&\sum_{i=0}^{l-1}\alpha_i(f_{x1}^1+f_{x1}^2)+\sum_{i=0}^{l-1}\beta_i f_{y1}+\sum_{i=0}^{l-1}\gamma_i f_{z1}=0\\
&\sum_{i=0}^{l-1}\alpha_i f_{x2}+\sum_{i=0}^{l-1}\beta_i(f_{y2}^1+f_{y2}^2)+\sum_{i=0}^{l-1}\gamma_i f_{z2}=0\\
&\sum_{i=0}^{l-1}\alpha_i f_{x3}+\sum_{i=0}^{l-1}\beta_i f_{y3}+\sum_{i=0}^{l-1}\gamma_i f_{z3}=-p_z
\end{aligned}\right\} \qquad (8a)$$

Here ,

$$
\left.
\begin{aligned}
f_{z1} &= \mu_1(\Lambda_2-\Lambda_1)\frac{\partial}{\partial x}w_z(x,y)G_i(x,y)\\
f_{z2} &= \mu_1(\Lambda_2-\Lambda_1)\frac{\partial}{\partial y}w_z(x,y)G_i(x,y)\\
f_{x3} &= \mu_1(\Lambda_2-\Lambda_1)\frac{\partial}{\partial x}w_x(x,y)G_i(x,y)\\
f_{y3} &= \mu_1(\Lambda_2-\Lambda_1)\frac{\partial}{\partial y}w_y(x,y)G_i(x,y)\\
f_{x1}^1 &= \mu_1\frac{2\Lambda-\Lambda_1-\Lambda_2}{2\pi}\int_s\frac{1}{r^3}w_x(\xi,\eta)G_i(\xi,\eta)ds(\xi,\eta)\\
f_{x1}^2 &= 3\mu_1\frac{\Lambda_1+\Lambda_2-\Lambda}{2\pi}\int_s\frac{(x-\xi)^2}{r^5}w_x(\xi,\eta)G_i(\xi,\eta)ds(\xi,\eta)\\
f_{y1} &= 3\mu_1\frac{\Lambda_1+\Lambda_2-\Lambda}{2\pi}\int_s\frac{(x-\xi)(y-\eta)}{r^5}w_y(\xi,\eta)G_i(\xi,\eta)ds(\xi,\eta)\\
f_{y2}^1 &= \mu_1\frac{2\Lambda-\Lambda_1-\Lambda_2}{2\pi}\int_s\frac{1}{r^3}w_y(\xi,\eta)G_i(\xi,\eta)ds(\xi,\eta)\\
f_{x2} &= 3\mu_1\frac{\Lambda_1+\Lambda_2-\Lambda}{2\pi}\int_s\frac{(x-\xi)(y-\eta)}{r^5}w_x(\xi,\eta)G_i(\xi,\eta)ds(\xi,\eta)\\
f_{y2}^2 &= 3\mu_1\frac{\Lambda_1+\Lambda_2-\Lambda}{2\pi}\int_s\frac{(y-\eta)^2}{r^5}w_y(\xi,\eta)G_i(\xi,\eta)ds(\xi,\eta)\\
f_{z3} &= \mu_1\frac{\Lambda_1+\Lambda_2}{2\pi}\int_s\frac{1}{r^3}w_z(\xi,\eta)G_i(\xi,\eta)ds(\xi,\eta)
\end{aligned}
\right\} \qquad (8b)
$$

where

$$
f_{z1} = \mu_1(\Lambda_2-\Lambda_1)\sum_{l=1}^{2}\frac{1+k_l}{4\mu_l\cosh\pi\varepsilon}\times\frac{1}{\sqrt{a^2-x^2}}\times
$$
$$
x^{-1+m}y^n\sqrt{b^2-y^2}\cos\left(\varepsilon\ln\left(\frac{b-y}{b+y}\right)\right)\times\left[\left(a^2m-(1+m)x^2\right)\cos\left(\varepsilon\ln\left(\frac{a-x}{a+x}\right)\right)+2a\varepsilon x\sin\left(\varepsilon\ln\left(\frac{a-x}{a+x}\right)\right)\right]
$$

$$
f_{z2} = \mu_1(\Lambda_2-\Lambda_1)\sum_{l=1}^{2}\frac{1+k_l}{4\mu_l\cosh\pi\varepsilon}\times\frac{1}{\sqrt{b^2-y^2}}\times
$$
$$
\left(y^{-1+n}x^m\sqrt{a^2-x^2}\cos\left(\varepsilon\ln\left(\frac{a-x}{a+x}\right)\right)\times\left[\left(b^2n-(1+n)y^2\right)\cos\left(\varepsilon\ln\left(\frac{b-y}{b+y}\right)\right)+2b\varepsilon y\sin\left(\varepsilon\ln\left(\frac{b-y}{b+y}\right)\right)\right]\right)
$$

$$
f_{x3} = \mu_1(\Lambda_2-\Lambda_1)\sum_{l=1}^{2}\frac{1+k_l}{4\mu_l\cosh\pi\varepsilon}\times\frac{1}{\sqrt{a^2-x^2}}\times
$$
$$
\left(x^{-1+m}y^n\sqrt{b^2-y^2}\cos\left(\varepsilon\ln\left(\frac{b-y}{b+y}\right)\right)\times\left[\left(a^2m-(1+m)x^2\right)\sin\left(\varepsilon\ln\left(\frac{a-x}{a+x}\right)\right)-2a\varepsilon x\cos\left(\varepsilon\ln\left(\frac{a-x}{a+x}\right)\right)\right]\right)
$$

$$
f_{y2} = \mu_1(\Lambda_2-\Lambda_1)\sum_{l=1}^{2}\frac{1+k_l}{4\mu_l\cosh\pi\varepsilon}\times\frac{1}{\sqrt{b^2-y^2}}\times
$$
$$
\left(y^{-1+n}x^m\sqrt{a^2-x^2}\cos\left(\varepsilon\ln\left(\frac{a-x}{a+x}\right)\right)\times\left[\left(b^2n-(1+n)y^2\right)\sin\left(\varepsilon\ln\left(\frac{b-y}{b+y}\right)\right)-2b\varepsilon y\cos\left(\varepsilon\ln\left(\frac{b-y}{b+y}\right)\right)\right]\right)
$$

(8c)

4 How to evaluate the hypersingular integrals

Each integral in Eq.(8) has a hypersingularity of the form r^{-3} when $x=\xi$ and $y=\eta$, and it cannot be evaluated in the present form. Using the Taylor's expansion with the local polar coordinates system $\xi-x=r\cos\theta$, $\eta-y=r\sin\theta$ as shown in Fig.3, the following expressions are given, and they will be applied to evaluate the integral.

Fig.3

$$\sqrt{a^2-\xi^2}=P_0(x)-(\xi-x)P_1(x)-(\xi-x)^2P_2(\xi,x) \tag{9a}$$

$$\sqrt{b^2-\eta^2}=Q_0(y)-(\eta-y)Q_1(y)-(\eta-y)^2Q_2(\eta,y) \tag{9b}$$

Here

$$P_0(x)=\sqrt{a^2-\xi^2},\qquad P_1(x)=\frac{x}{\sqrt{a^2-x^2}},$$

$$P_2(\xi,x)=\frac{\xi+x}{\sqrt{a^2-x^2}\left(\sqrt{a^2-\xi^2}+\sqrt{a^2-x^2}\right)}\times\frac{a^2}{\left(\xi\sqrt{a^2-x^2}+x\sqrt{a^2-\xi^2}\right)}$$

$$Q_0(x)=\sqrt{b^2-\eta^2}\qquad Q_1(y)=\frac{y}{\sqrt{b^2-y^2}}$$

$$Q_2(\eta,y)=\frac{\eta+y}{\sqrt{b^2-y^2}\left(\sqrt{b^2-\eta^2}+\sqrt{b^2-y^2}\right)}\times\frac{b^2}{\left(\eta\sqrt{b^2-y^2}+y\sqrt{b^2-\eta^2}\right)}$$

$$\begin{aligned}\xi^m&=x^m+mx^{m-1}(\xi-x)+\sum_{i=0}^{m-2}\left[(i+1)\xi^{(m-2-i)}x^i\right](\xi-x)^2\\&=b_0(x)+b_1(x)(\xi-x)+b_2(\xi,x)(\xi-x)^2\end{aligned} \tag{9c}$$

$$\eta^n = x^n + nx^{n-1}(\eta - y) + \sum_{i=0}^{n-2}\left[(i+1)\eta^{(n-2-i)}y^i\right](\eta - y)^2 \qquad (9d)$$
$$= c_0(y) + c_1(y)(\eta - y) + c_2(\eta, y)(\eta - y)^2$$

$$FC_{11} = \cos\left(\varepsilon \ln(\frac{a-\xi}{a+\xi})\right) = R_{01}(x) + R_{11}(x)(\xi - x) + R_{21}(x)(\xi - x)^2 \qquad (9e)$$

$$FS_{11} = \sin\left(\varepsilon \ln(\frac{a-\xi}{a+\xi})\right) = R_{02}(x) + R_{12}(x)(\xi - x) + R_{22}(x)(\xi - x)^2 \qquad (9f)$$

$$FC_{21} = \cos\left(\varepsilon \ln(\frac{b-\eta}{b+\eta})\right) = T_{01}(y) + T_{11}(y)(\eta - y) + T_{21}(y)(\eta - y)^2 \qquad (9g)$$

$$FS_{21} = \sin\left(\varepsilon \ln(\frac{b-\eta}{b+\eta})\right) = T_{02}(y) + T_{12}(y)(\eta - y) + T_{22}(y)(\eta - y)^2 \qquad (9h)$$

Here

$$R_{01} = \cos\left(\varepsilon \ln(\frac{a-x}{a+x})\right) \ , \ R_{02} = \sin\left(\varepsilon \ln(\frac{a-x}{a+x})\right),$$

$$T_{01} = \cos\left(\varepsilon \ln(\frac{b-y}{b+y})\right) \ , \ T_{02} = \sin\left(\varepsilon \ln(\frac{b-y}{b+y})\right),$$

$$R_{11}(x) = \frac{2a\varepsilon}{a^2 - x^2}R_{02} \ , \ R_{12}(x) = -\frac{2a\varepsilon}{a^2 - x^2}R_{01} \ , \ T_{11}(y) = \frac{2b\varepsilon}{b^2 - y^2}T_{02} \ , \ T_{12}(y) = -\frac{2b\varepsilon}{b^2 - y^2}T_{01},$$

$$R_{21}(x) =$$
$$\begin{cases} \dfrac{1}{(\xi - x)^2}\left(FC_{11} - R_{01}(x) - R_{11}(x)(\xi - x)\right) & |x - \xi| \geq \varepsilon_0 \\ \dfrac{2a\varepsilon x}{\left(a^2 - x^2\right)^2}R_{02} - \dfrac{2a^2\varepsilon^2}{\left(a^2 - x^2\right)^2}R_{01} & |x - \xi| \leq \varepsilon_0 \end{cases},$$

$$R_{22}(x) =$$
$$\begin{cases} \dfrac{1}{(\xi - x)^2}\left(FS_{11} - R_{02}(x) - R_{12}(x)(\xi - x)\right) & |x - \xi| \geq \varepsilon_0 \\ \dfrac{2a\varepsilon x}{\left(a^2 - x^2\right)^2}R_{01} - \dfrac{2a^2\varepsilon^2}{\left(a^2 - x^2\right)^2}R_{02} & |x - \xi| \leq \varepsilon_0 \end{cases}$$

$$T_{21}(y) =$$
$$\begin{cases} \dfrac{1}{(\eta - y)^2}\left(FC_{21} - T_{01}(y) - T_{11}(y)(\eta - y)\right) & |y - \eta| \geq \varepsilon_0 \\ \dfrac{2b\varepsilon y}{\left(b^2 - y^2\right)^2}T_{02} - \dfrac{2b^2\varepsilon^2}{\left(b^2 - y^2\right)^2}T_{01} & |y - \eta| \leq \varepsilon_0 \end{cases},$$

$$T_{22}(y)=\begin{cases}\dfrac{1}{(\eta-y)^2}\left(FS_{21}-T_{02}(y)-T_{12}(y)(\eta-y)\right) & |y-\eta|\geq\varepsilon_0\\ \dfrac{2b\varepsilon y}{\left(b^2-y^2\right)^2}T_{01}-\dfrac{2b^2\varepsilon^2}{\left(b^2-y^2\right)^2}T_{02} & |y-\eta|\leq\varepsilon_0\end{cases} \tag{9i}$$

In the numerical calculation, we may put $\varepsilon_0=10^{-10}$ in Eq. (9i). Using the concept of finite-part integral method and the relations (9a)-(9i), the hypersingular integral in Eq. (8) can be reduced to the following form.

$$\begin{aligned}I_{mn}(x,y)&=\int_0^{2\pi}\int_0^{R(\theta)}\left[\frac{D_0(x,y)}{r^2}+\frac{D_1(\theta)}{r}\right]\mathrm{d}r\,\mathrm{d}\theta+\int_0^{2\pi}\int_0^{R(\theta)}D_2(r,\theta)\,\mathrm{d}r\,\mathrm{d}\theta\\&=\int_0^{2\pi}\left[-\frac{D_0(x,y)}{R(\theta)}+D_1(x,y,\theta)\ln(R(\theta))+\int_0^{R(\theta)}D_2(x,y,r,\theta)\mathrm{d}r\right]\mathrm{d}\theta\end{aligned} \tag{10}$$

In Eq. (10), $D_0(x,y)$, $D_1(x,y,\theta)$ and $D_2(x,y,r,\theta)$ are known functions, which can be expressed as a combination of Eq. (9). Now the integral in (10) is general, and can be calculated numerically. The notation $R(\theta)$ means a distance between a point (x,y) in question and a point on the fictitious boundary of the crack as shown in Fig.3.

5 Numerical results and discussion

Consider a rectangular interface crack in three-dimensional infinite elastic solid under remote uniform tension $\sigma_z^{\infty}=1$. Numerical

integrals have been performed very accurately using double exponential type formulas; for example, scientific subroutine library FACOM SSL2 DAQME. In demonstrating the numerical results of stress intensity factors (SIFs), the following dimensionless factors F_I, F_{II}, F_{III} will be used. Here, the SIFs F_I, F_{II}, F_{III} are expressed on the basis of the SIF of 2D interface crack whose length is 2b.

$$F_I + iF_{II} = \frac{K_I(x,y)\big|_{y=\pm b} + iK_{II}(x,y)\big|_{y=\pm b}}{\sigma_z^{\infty}\sqrt{\pi b}} = \sqrt{a^2 - x^2}\left(\cos\left(\varepsilon \ln(\frac{a-x}{a+x})\right)F_z(x,y)\big|_{y=\pm b} + 2i\varepsilon F_y(x,y)\big|_{y=\pm b}\right)$$

$$F_{III} = \frac{K_{III}(x,y)\big|_{y=\pm b}}{\sigma_z^{\infty}\sqrt{\pi b}} = \sum_{l=1}^{2} \frac{1+\kappa_l}{4\mu_l \cosh \pi\varepsilon} \frac{1}{(1/\mu_1 + 1/\mu_2)} \sqrt{a^2 - x^2} \sin\left(\varepsilon \ln(\frac{a-x}{a+x})\right) F_x\big|_{y=\pm b}$$

(11)

5.1 Compliance of boundary condition and convergence of numerical solutions

Figure 4 (a)-(c) show the compliance of boundary condition along

Fig.4

the crack surface for a/b=1, $\nu_1 = \nu_2 = 0.3$, $\varepsilon = 0.02$ when the collocation

point number is 100(10×10). Here, the boundary conditions are considered at the intersection of the mesh 10×10 when the polynomial exponents m and n in Eq. (8) are changed as m=n=6 and m=n=8. In solving the algebraic equation (8), the least square regression method is applied to minimize the residual stress at the collocation points. It is seen that the remaining stresses $(\frac{\sigma_z}{\sigma_z^\infty}+1)$, $\frac{\tau_{yz}}{\sigma_z^\infty}$, $\frac{\tau_{zx}}{\sigma_z^\infty}$ on the fictitious boundary of the crack are less than 4.4×10^{-5} when $m=n$=6, less than 1.5×10^{-6}, when $m=n$=8.

For the crack in homogeneous materials, the results of dimensionless stress intensity factors are shown in Table 1 with varying the polynomial exponents when the collocation point is

Table 1, Table 2

10×10 , a/b=1, $\nu_1=\nu_2=0.3$. The results coincide with the previous results given by Wang et al (2001) and Qin et al (2003). Table 2 shows the results of ε=0.02 when the collocation point is 10×10 , a/b=1,and $\nu_1=\nu_2=0.3$. From Table 1 and Table 2, it is seen that the present method gives the results with good convergence.

5.2 Comparison with the two-dimension case

For large aspect ratio a/b, the results should coincide with the two-dimensional solution. For a/b=8 the stress intensity factor of crack are given in Table3 when the polynomial exponents $m=n$=8 and the collocation point number is 10×10. It is seen that

Table 3

the present results coincide with the two-dimensional exact solution known as $F_I=1, F_{II}=2\varepsilon$, $F_{III}=0$ when $a/b\to\infty$.

5.3 Solutions for general cases

For general cases, the following results are given. Here, the polynomial exponents are taken as $m=n$=8 with the collocation point number 10×10. The distributions of the stress intensity factor F_I and F_{II} are shown in Table 4 with varying ε when a/b=1. It is seen

Table 4

that the stress intensity factor F_I decreases with increasing ε, and F_{II} increases with increasing of ε. The maximum stress intensity

factors are compared with the results of a penny-shaped interface crack in Table5. The F_I values of a square interface crack are larger than the results of a penny-shaped interface crack, and F_{II} values are smaller. The maximum stress intensity factor F_I and F_{II} for a rectangular interface crack at the point $(x, y) = (0, b)$ are given in Table6 for a/b=1, 2, 4, 8.

Table 5, Table 6

5.4 Stress intensity factors are controlled by ε alone

The stress intensity factors F_I, F_{II}, F_{III} are indicated in Table7 for a/b=1 and ε=0.02 for various Poisson's ratio and shear modulus ratio.

Table 7, Table 8, Table 9

Also, the results for a/b=1 and ε=0.04 are indicated in Tables 8, and the results for a/b=2 and ε=0.02 are given in Table 9. From

Table 7, Table 8, Table 9

these tables, it is found that F_I and F_{II} values are constant and independent of the shear modulus ratio μ_2/μ_1 and Poisson's ratio if ε is constant. In other words, the stress intensity factors K_I and K_{II} of planer interface cracks in bimaterials are determined by the bimaterial constant ε alone, independent of the shear modulus ratio and Poisson's ratio, and of course, Young's modulus ratio. The F_{III} values is smaller than the values F_I and F_{II}, and in the range, $F_{III\max} \le 10^{-2} \times F_{I\max}$, and $F_{III\max} \le 0.5 \times F_{II\max}$. The maximum value of F_{III} appears at a point that is very close to the corner of the rectangle.

6 Conclusions

In this study a planar rectangular interfacial crack in three-dimensional bimaterials was considered through the singular integral equations on the basis of the body force method. The conclusion can be summarized as follows:

(1) The unknown functions of the singular integral equations are approximated by using fundamental density functions and polynomials. Here, the fundamental densities are chosen to express the singular behavior of the stresses around the crack front exactly. The numerical results show that this numerical technique is successful, and the

boundary conditions are satisfied precisely.

(2) For the large aspect ratio $a/b \geq 8$, the stress intensity factors at the center of the crack front coincide with the two-dimension results.

(3) Dimensionless stress intensity factors F_I and F_{II} were found to be constant for the variation of the shear modulus ratio μ_2/μ_1 and Poisson's ratio ν_1, $\nu_2 = 0 \sim 0.5$, if ε is constant. In other words, the stress intensity factors K_I and K_{II} of planer interface cracks in bimaterials are determined by the bimaterial constant ε alone, independent of the shear modulus ratio and Poisson's ratio, and of course, Young's modulus ratio.

(4) The F_{III} values is smaller than the values F_I and F_{II}, and in the range, $F_{III\max} \leq 10^{-2} \times F_{I\max}$, and $F_{III\max} \leq 0.5 \times F_{II\max}$. The maximum value of F_{III} appears at a point that is very close to the corner of the rectangle.

This research was supported by Japanese Government (Monbukagakusho) Scholarship. The authors wish to express their thanks to the member of their group, especially Mr Yasushi Takase, who carried our much of constructional works.

References

Chen M. C. Noda, N. A., and Tang, R. J., 1999, “Application of Finite-part Integrals to Planar Interfacial Fracture Problems in Three Dimensional Bimaterials”, Trans. ASME J. Appl. Mech., 66, pp.885-890.

Comninou, M., 1977, “The Interface Crack, ” Trans. ASME J. Appl. Mech., 44, pp.631-636.

England, A.H., 1965, “A Crack between Dissimilar Media, ” Trans. ASME J. Appl. Mech., 32, pp. 400-402.

Erdogan, F., 1963, “Stresses Distribution in a Non-homogeneous Elastic Plane with Crack,” Trans. ASME J. Appl. Mech., 30, pp. 232-236.

Erdogan, F., 1965, “Stress Distribution in Bonded Dissimilar Materials Containing Circular or Ring-Shaped Cavities, ” Trans. ASME, J. Appl. Mech., 32, pp.403-410.

Erdogan, F., and Gupta, G. D., 1975, “Bonded Wedges with an Interface Crack under Anti-Plane Shear Loading,” Int. J. Fract., 11, pp.593-593.

Hadamard, J., 1923, “Lectures on Cauchy’s Problem in Linear Partial Differential Equations”, Yale University Press.

Kassir, M. K. and Bregman, A. M., 1972, “The Stress Intensity Factor for a Penny-Shaped Crack between Two Dissimilar Materials, ” Trans. ASME. J. Appl. Mech., 39, pp.308-310.

Lowengrub, M., and Senddon, I. N., 1974, “The Effect of Internal Pressure on a Penny-Shaped Crack at the Interface of Two Bonded Dissimilar Elastic Half-Spaces, ” Int. J. Eng. Sci., 12, pp.387-396.

Mossakovski, V. I., and Rybka, M. T., 1964, “Generalization of the Griffith-Senddon Criterion for the Case of a Non-homogeneous Body, ” Prikl. Mat. Mekh., 28, pp.1061-1069.

Nisitani, H., 1967, “The two-Dimensional Stress Problem Solved Using an Electric Digital Computer,” Journal of the Japan Society of

Mechanical Engineers 11, pp.627-632. (in Japanese). [1968. Bulletin of Japan Society of Mechanical Engineers 11, 14-23.]

Nisitani, H., and Murakami, Y., 1974, “Stress Intensity Factor of an Elliptical Crack and a Semi-Elliptical Crack in Plates Subjected to Tension”, Int. J. Fracture, 10, pp.353-368.

Nisitani, H., Saimoto, A., Noguchi, H., 1993, “Analysis of an Interface Crack Based on the Body Force Method”, Trans. Japan. Soc. Mechanical Engineers, Ser.A, 59, pp.68-73 (in Japanese).

Noda, N. A., Kagita, M., and Chen, M. C., 2003, “Analysis of Stress Intensity Factors of a Ring-Shaped Interface Crack, ” Int. J. Solids and Structures. 40. pp.6577-6592.

Noda, N.A. and Matsuo, T., 1998, “Singular Integral Equation Method for Interaction between Elliptical Inclusions”, Trans. ASME Journal of Applied Mechanics 65, pp.310-319.

Noda, N.A. and Oda, K., 1992, “Numerical Solutions of the Singular Integral Equations in the Crack Analysis Using the Body Force

Method", International Journal of Fracture, 58, pp.285-304.

Noda, N.A., and Miyoshi, S., 1996, "Variation of Stress Intensity Factors and Crack Opening Displacement of Semi-elliptical Surface Crack, " Int. J. Fract., 75,pp.19-48.

Noda, N.A. and Oda, K., 1997, "Interaction Effect of Stress Intensity Factors for any Number of Collinear Interface Cracks, " Int. J. Fract., 84, pp.117-128.

Qin, T.Y. and Noda, N. A., 2003, "Stress Intensity Factors of Rectangular Crack Meeting a Bimateral Interface, " Int. J. Solids Struct., 40, pp. 2473-2486.

Rice, J. R. and Sih, G. C., 1965, "Plane Problems of Cracks in Dissimilar Media, " Trans. ASME, J. Appl. Mech., 32, pp. 418-423.

Salganik, R.L., 1963, "The Brittle Fracture of Cemented Bodies," Prikl. Mat. Mekh., 27, pp. 957-962.

Shibuya, T., Koizumi, T., and Iwamoto, T., 1989, “Stress Analysis of the Vicinity of an Elliptical Crack at the Interface of Two Bonded Half-Spaces, ” JSME Int. J., 32, pp.485-491.

Tucker, M. O., 1974, “In Two-phase Solids under Longitudinal Shear Loading, ” Int. J. Fract., 10, pp. 323-336.

Willis, J.R., 1971, “Fracture Mechanics of Interfacial Crack, ” J. Mech. Phys. Solids., 19, pp.353-368.

Willis, J.R., 1972, “The Penny-Shaped Crack on an Interface, ” J. Mech. Appl. Math., 25, pp.367-385.

Wang, Q., Noda, N. A., Honda, M., and Chen, M.C., 2001, “Variation of Stress Intensity Factors along the Front of 3D Rectangular Crack by Using a Singular Integral Equation Method, ” Int. J. Fract., 108, pp.119-131.

Table headings

Table1 Convergence of stress intensity factor F_I at $y=b$ for ε=0, a/b=1

Table2 Convergence of stress intensity factor at $y=b$ for ε=0.02, a/b=1 (a) F_I, (b) F_{II}, (c) F_{III}

Table3 Dimensionless stress intensity factor at $y=b$ for $a/b=8$ (a) F_I, (b) F_{II}, (c) F_{III}

Table4 stress intensity factor F_1 at y=b for a/b=1 (a) F_I, (b) F_{II}

Table5 Comparison with the results of disk interface crack ($\nu_1=\nu_2=0.3$)

Table6 Dimensionless stress intensity factor at the point (0,1)

Table7 stress intensity factor at y=b for a/b=1, ε=0.02 (a) F_I, (b) F_{II}, (c) F_{III}

Table8 Stress intensity factor for a/b=2, ε=0.02 (a) F_I, (b) F_{II}

Table9 Stress intensity factor for a/b=1, ε=0.04 (a) F_I, (b) F_{II}

Figure captions

Fig.1 Problem configuration

Fig2. Fundamental densities for two dimensional problems

Fig.3 Integral parameters

Fig.4 Compliance of boundary condition for $a/b=1, \varepsilon=0.02$

Table1 Convergence of stress intensity factor F_I at $y=b$ for ε=0, a/b=1

x/a	0/11	1/11	2/11	3/11	4/11	5/11	6/11	7/11	8/11	9/11	10/11
$m=n$ =4	0.7521	0.7507	0.7462	0.7379	0.7250	0.7066	0.6821	0.6509	0.6108	0.5538	0.4497
$m=n$ =6	0.7538	0.7520	0.7467	0.7377	0.7248	0.7072	0.6836	0.6520	0.6094	0.5482	0.4423
$m=n$ =8	0.7534	0.7516	0.7463	0.7373	0.7243	0.7063	0.6821	0.6500	0.6081	0.5513	0.4543
Qin	0.7534	0.7512	0.7462	0.7379	0.7255	0.7072	0.6821	0.6497	0.6090	0.5521	0.4464
Wang	0.7534	0.7517	0.7465	0.7376	0.7245	0.7066	0.6828	0.6512	0.6086	0.5492	0.4536

Table2 Convergence of stress intensity factor at $y=b$ for ε=0.02, a/b=1

(a) Stress intensity factor F_I

x/a	0/11	1/11	2/11	3/11	4/11	5/11	6/11	7/11	8/11	9/11	10/11
$m=n$ =4	0.7531	0.7512	0.7457	0.7364	0.7233	0.7059	0.6828	0.6517	0.6073	0.5385	0.4177
$m=n$ =6	0.7524	0.7507	0.7456	0.7367	0.7237	0.7060	0.6826	0.6519	0.6098	0.5465	0.4329
$m=n$ =8	0.7528	0.7511	0.7459	0.7369	0.7238	0.7058	0.6822	0.6514	0.6099	0.5490	0.4400

(b) Stress intensity factor F_{II}

x/a	0/11	1/11	2/11	3/11	4/11	5/11	6/11	7/11	8/11	9/11	10/11
$m=n$ =4	0.0272	0.0271	0.0268	0.0264	0.0257	0.0248	0.0236	0.0221	0.0200	0.0171	0.0127
$m=n$ =6	0.0273	0.0272	0.0270	0.0265	0.0259	0.0250	0.0238	0.0223	0.0203	0.0174	0.0131
$m=n$ =8	0.0274	0.0273	0.0271	0.0266	0.0260	0.0251	0.0239	0.0224	0.0203	0.0176	0.0133

(c) Stress intensity factor F_{III}

x/a	0/11	1/11	2/11	3/11	4/11	5/11	6/11	7/11	8/11	9/11	10/11
$m=n$ =4	0	0.0010	0.0021	0.0031	0.0042	0.0053	0.0065	0.0079	0.0094	0.0109	0.0120
$m=n$ =6	0	0.0010	0.0020	0.0031	0.0041	0.0052	0.0064	0.0076	0.0091	0.0106	0.0120
$m=n$ =8	0	0.0010	0.0020	0.0031	0.0041	0.0051	0.0063	0.0075	0.0089	0.0105	0.0120

Table3 Dimensionless stress intensity factor at $y=b$ for $a/b=8$

(a) Stress intensity factor F_I

x/a	0/11	1/11	2/11	3/11	4/11	5/11	6/11	7/11	8/11	9/11	10/11
ε=0.02	0.9947	0.9946	0.9942	0.9933	0.9917	0.9888	0.9838	0.9750	0.9580	0.9175	0.7954
ε=0.04	0.9938	0.9937	0.9932	0.9923	0.9907	0.9878	0.9828	0.9739	0.9568	0.9160	0.7931
ε=0.06	0.9920	0.9919	0.9914	0.9905	0.9889	0.9860	0.9809	0.9719	0.9545	0.9134	0.7892
ε=0.08	0.9891	0.9890	0.9885	0.9875	0.9859	0.9830	0.9779	0.9687	0.9509	0.9092	0.7836
ε=0.10	0.9848	0.9847	0.9842	0.9833	0.9816	0.9786	0.9733	0.9640	0.9461	0.9037	0.7755

(b) Stress intensity factor F_{II}

x/a	0/11	1/11	2/11	3/11	4/11	5/11	6/11	7/11	8/11	9/11	10/11
ε=0.02	0.0397	0.0397	0.0396	0.0396	0.0395	0.0394	0.0391	0.0387	0.0378	0.0359	0.0304
ε=0.04	0.0786	0.0786	0.0785	0.0784	0.0783	0.0780	0.0775	0.0766	0.0749	0.07107	0.0601
ε=0.06	0.1160	0.1160	0.1160	0.1158	0.1156	0.1152	0.1144	0.1131	0.1106	0.1047	0.0885
ε=0.08	0.1515	0.1515	0.1514	0.1512	0.1509	0.1503	0.1493	0.1476	0.1442	0.1364	0.1151
ε=0.10	0.1845	0.1845	0.1844	0.1842	0.1838	0.1831	0.1819	0.1797	0.1755	0.1658	0.1394

(c) Stress intensity factor $F_{III}\times10^2$

x/a	0/11	1/11	2/11	3/11	4/11	5/11	6/11	7/11	8/11	9/11	10/11
ε=0.02	0	0.0609	0.1217	0.1823	0.2423	0.3013	0.3584	0.4118	0.4579	0.4793	0.4887
ε=0.04	0	0.1086	0.2371	0.3551	0.4721	0.5872	0.6985	0.8028	0.8932	0.9370	0.9540
ε=0.06	0	0.1704	0.3406	0.5101	0.6784	0.8439	1.004	1.155	1.286	1.354	1.375
ε=0.08	0	0.2141	0.4279	0.6411	0.8562	1.061	1.263	1.453	1.620	1.714	1.736
ε=0.10	0	0.2484	0.4965	0.7439	0.9897	1.232	1.467	1.690	1.886	2.009	2.026

Table4 Stress intensity factor at y=b for a/b=1, $\nu_1 = \nu_2 = 0.3$

(a) Stress intensity factor F_I

x/a	0/11	1/11	2/11	3/11	4/11	5/11	6/11	7/11	8/11	9/11	10/11
ε =0	0.7534	0.7516	0.7463	0.7373	0.7243	0.7063	0.6821	0.6500	0.6081	0.5513	0.4543
ε =0.02	0.7528	0.7511	0.7459	0.7369	0.7238	0.7058	0.6822	0.6514	0.6099	0.5490	0.4400
ε =0.04	0.7509	0.7492	0.7440	0.7351	0.7219	0.7040	0.6804	0.6495	0.6080	0.5470	0.4377
ε =0.06	0.7478	0.7461	0.7409	0.7320	0.7188	0.7009	0.6773	0.6464	0.6048	0.5436	0.4339
ε =0.08	0.7433	0.7416	0.7364	0.7275	0.7143	0.6965	0.6729	0.6419	0.6003	0.5389	0.4286
ε =0.10	0.7373	0.7356	0.7304	0.7215	0.7085	0.6906	0.6671	0.6362	0.5945	0.5329	0.4218

(b) Stress intensity factor F_{II}

x/a	0/11	1/11	2/11	3/11	4/11	5/11	6/11	7/11	8/11	9/11	10/11
ε =0.02	0.0274	0.0273	0.0271	0.0266	0.0260	0.0251	0.0239	0.0224	0.0204	0.0176	0.0133
ε =0.04	0.0542	0.0540	0.0535	0.0527	0.0514	0.0497	0.0474	0.0443	0.0403	0.0349	0.0365
ε =0.06	0.0798	0.0796	0.0789	0.0777	0.0758	0.0733	0.0699	0.0654	0.0595	0.0515	0.0392
ε =0.08	0.1040	0.1037	0.1028	0.1012	0.0988	0.0955	0.0911	0.0853	0.0776	0.0673	0.0514
ε =0.10	0.1263	0.1259	0.1248	0.1229	0.1201	0.1161	0.1107	0.1037	0.0945	0.0821	0.0629

Table5 Comparison with the results of a penny-shaped interface crack ($\nu_1 = \nu_2 = 0.3$ **)**

	F_I		F_{II}	
	square	penny	square	penny
ε =0.02	0.7528	0.636	0.0274	0.030
ε =0.04	0.7509	0.636	0.0542	0.061
ε =0.06	0.7478	0.635	0.0799	0.091
ε =0.08	0.7433	0.634	0.1040	0.122
ε =0.10	0.7373	0.632	0.1263	0.152

Table6 Dimensionless stress intensity factor F_I and F_{II} at the point $(x, y) = (0, b)$ in Fig.1(b)

	F_I				F_{II}			
	a/b=1	a/b=2	a/b=4	a/b=8	a/b=1	a/b=2	a/b=4	a/b=8
ε =0.02	0.7528	0.9052	0.9760	0.9947	0.0274	0.0352	0.0388	0.0397
ε =0.04	0.7509	0.9038	0.9750	0.9938	0.0542	0.0696	0.0768	0.0786
ε =0.06	0.7478	0.9013	0.9730	0.9920	0.0799	0.1027	0.1134	0.1160
ε =0.08	0.7433	0.8975	0.9699	0.9891	0.1040	0.1338	0.1479	0.1515
ε =0.10	0.7373	0.8921	0.9654	0.9848	0.1263	0.1627	0.1801	0.1845

Table7 Stress intensity factor at y=b for a/b=1, ε =0.02

(a) Stress intensity factor F_I

ν_1	ν_2	μ_2 / μ_1	0/11	1/11	2/11	3/11	4/11	5/11	6/11	7/11	8/11	9/11	10/11
0	0	1.2870	0.7528	0.7511	0.7459	0.7370	0.7238	0.7059	0.6822	0.6513	0.6099	0.5490	0.4400
0	0.1	1.0439	0.7528	0.7511	0.7459	0.7369	0.7238	0.7059	0.6822	0.6513	0.6099	0.5490	0.4400
0	0.2	0.8009	0.7528	0.7511	0.7459	0.7369	0.7238	0.7058	0.6822	0.6513	0.6099	0.5490	0.4400
0	0.3	0.5578	0.7528	0.7511	0.7459	0.7369	0.7238	0.7058	0.6822	0.6514	0.6099	0.5490	0.4400
0	0.4	0.3148	0.7528	0.7511	0.7459	0.7369	0.7238	0.7058	0.6822	0.6514	0.6099	0.5490	0.4400
0	0.5	0.0718	0.7527	0.7511	0.7459	0.7369	0.7238	0.7058	0.6822	0.6514	0.6099	0.5490	0.4400
0.1	0.1	1.3288	0.7528	0.7511	0.7459	0.7369	0.7238	0.7059	0.6822	0.6514	0.6099	0.5490	0.4400
0.1	0.2	1.0194	0.7528	0.7511	0.7459	0.7369	0.7238	0.7058	0.6822	0.6514	0.6099	0.5490	0.4400
0.1	0.3	0.7101	0.7528	0.7511	0.7459	0.7369	0.7238	0.7058	0.6822	0.6514	0.6099	0.5490	0.4400
0.1	0.4	0.4007	0.7528	0.7511	0.7459	0.7369	0.7238	0.7058	0.6822	0.6514	0.6099	0.5490	0.4400
0.1	0.5	0.0913	0.7527	0.7511	0.7459	0.7369	0.7238	0.7058	0.6822	0.6514	0.6099	0.5490	0.4400
0.2	0.2	1.4019	0.7528	0.7511	0.7459	0.7369	0.7238	0.7058	0.6822	0.6514	0.6099	0.5490	0.4400
0.2	0.3	0.9765	0.7528	0.7511	0.7459	0.7369	0.7238	0.7058	0.6822	0.6514	0.6099	0.5490	0.4400
0.2	0.4	0.5510	0.7528	0.7511	0.7459	0.7369	0.7238	0.7058	0.6822	0.6514	0.6099	0.5490	0.4400
0.2	0.5	0.1256	0.7527	0.7511	0.7459	0.7369	0.7238	0.7058	0.6822	0.6514	0.6099	0.5490	0.4400
0.3	0.3	1.5628	0.7528	0.7511	0.7459	0.7369	0.7238	0.7058	0.6822	0.6514	0.6099	0.5490	0.4400
0.3	0.4	0.8819	0.7528	0.7511	0.7459	0.7369	0.7238	0.7058	0.6822	0.6514	0.6099	0.5490	0.4400
0.3	0.5	0.2010	0.7527	0.7511	0.7459	0.7369	0.7238	0.7058	0.6822	0.6514	0.6099	0.5490	0.4400
0.4	0.4	2.2076	0.7527	0.7511	0.7459	0.7369	0.7238	0.7058	0.6822	0.6514	0.6099	0.5490	0.4400
0.4	0.5	0.5032	0.7527	0.7511	0.7459	0.7369	0.7238	0.7058	0.6822	0.6514	0.6099	0.5490	0.4400
0.4999	0.4999	→0	0.7527	0.7511	0.7459	0.7369	0.7328	0.7058	0.6822	0.6514	0.6099	0.5490	0.4400

(b) Stress intensity factor F_{II}

ν_1	ν_2	μ_2/μ_1	0/11	1/11	2/11	3/11	4/11	5/11	6/11	7/11	8/11	9/11	10/11
0	0	1.2870	0.0278	0.0277	0.0274	0.0269	0.0262	0.0253	0.0241	0.0224	0.0202	0.0171	0.0122
0	0.1	1.0439	0.0277	0.0277	0.0274	0.0269	0.0262	0.0253	0.0241	0.0224	0.0203	0.0172	0.0124
0	0.2	0.8009	0.0277	0.0276	0.0273	0.0268	0.0262	0.0252	0.0240	0.0224	0.0203	0.0173	0.0126
0	0.3	0.5578	0.0276	0.0275	0.0272	0.0268	0.0260	0.0252	0.0240	0.0224	0.0203	0.0174	0.0129
0	0.4	0.3148	0.0274	0.0273	0.0271	0.0266	0.0260	0.0251	0.0239	0.0224	0.0204	0.0176	0.0134
0	0.5	0.0718	0.0271	0.0270	0.0268	0.0264	0.0258	0.0250	0.0238	0.0223	0.0204	0.0178	0.0141
0.1	0.1	1.3288	0.0277	0.0276	0.0273	0.0268	0.0262	0.0252	0.0240	0.0224	0.0203	0.0173	0.0126
0.1	0.2	1.0194	0.0276	0.0275	0.0273	0.0268	0.0261	0.0252	0.0240	0.0224	0.0203	0.0173	0.0127
0.1	0.3	0.7101	0.0275	0.0274	0.0272	0.0267	0.0261	0.0252	0.0240	0.0224	0.0203	0.0174	0.0130
0.1	0.4	0.4007	0.0274	0.0273	0.0270	0.0266	0.0260	0.0251	0.0239	0.0224	0.0204	0.0176	0.0134
0.1	0.5	0.0913	0.0271	0.0270	0.0268	0.0264	0.0258	0.0250	0.0238	0.0223	0.0204	0.0178	0.0141
0.2	0.2	1.4019	0.0275	0.0274	0.0272	0.0267	0.0261	0.0252	0.0240	0.0224	0.0203	0.0174	0.0129
0.2	0.3	0.9765	0.0275	0.0274	0.0271	0.0267	0.0260	0.0251	0.0240	0.0224	0.0204	0.0175	0.0131
0.2	0.4	0.5510	0.0273	0.0272	0.0270	0.0266	0.0260	0.0251	0.0239	0.0224	0.0204	0.0176	0.0135
0.2	0.5	0.1256	0.0271	0.0270	0.0268	0.0264	0.0258	0.0250	0.0238	0.0223	0.0203	0.0178	0.0141
0.3	0.3	1.5628	0.0274	0.0273	0.0271	0.0266	0.0260	0.0251	0.0239	0.0224	0.0204	0.0176	0.0134
0.3	0.4	0.8819	0.0273	0.0272	0.0270	0.0266	0.0259	0.0251	0.0239	0.0224	0.0204	0.0177	0.0136
0.3	0.5	0.2010	0.0271	0.0270	0.0268	0.0264	0.0258	0.0250	0.0238	0.0223	0.0204	0.0178	0.0141
0.4	0.4	2.2076	0.0272	0.0271	0.0269	0.0265	0.0259	0.0250	0.0239	0.0224	0.0204	0.0177	0.0138
0.4	0.5	0.5032	0.0271	0.0270	0.0268	0.0264	0.0258	0.0250	0.0238	0.0223	0.0204	0.0178	0.0141
0.4999	0.4999	$\to 0$	0.0271	0.0270	0.0268	0.0264	0.0258	0.0250	0.0238	0.0223	0.0204	0.0178	0.0141

(c) Stress intensity factor $F_{III} \times 10^{-2}$

ν_1	ν_2	μ_2/μ_1	0/11	1/11	2/11	3/11	4/11	5/11	6/11	7/11	8/11	9/11	10/11
0.3	0.3	1.5628	0	0.1010	0.2028	0.3061	0.4115	0.5199	0.6331	0.7545	0.8913	1.051	1.204
0.0	0.5	0.0718	0	0.0869	0.1746	0.2637	0.3550	0.4500	0.5517	0.6662	0.8011	0.9592	1.099
0.0	0.0	1.2870	0	0.1204	0.2415	0.3641	0.4884	0.6141	0.7400	0.8667	1.000	1.156	1.328

Table8 Stress intensity factor for a/b=2, ε=0.02

(a) Stress intensity factor F_I

ν_1	ν_2	μ_2/μ_1	0/11	1/11	2/11	3/11	4/11	5/11	6/11	7/11	8/11	9/11	10/11
0.3	0.3	1.5628	0.9052	0.9038	0.8993	0.8912	0.8791	0.8618	0.8381	0.8057	0.7601	0.6899	0.5583
0	0.5	0.0718	0.9052	0.9038	0.8992	0.8912	0.8791	0.8618	0.8381	0.8057	0.7601	0.6900	0.5584
0	0	1.2870	0.9053	0.9038	0.8993	0.8913	0.8791	0.8619	0.8381	0.8057	0.7601	0.6899	0.5582

(b) Stress intensity factor F_{II}

ν_1	ν_2	μ_2/μ_1	0/11	1/11	2/11	3/11	4/11	5/11	6/11	7/11	8/11	9/11	10/11
0.3	0.3	1.5628	0.0352	0.0351	0.0349	0.0345	0.0338	0.0330	0.0318	0.0302	0.0280	0.0246	0.0189
0	0.5	0.0718	0.0349	0.0348	0.0346	0.0342	0.0336	0.0328	0.0317	0.0301	0.0280	0.0248	0.0193
0	0	1.2870	0.0355	0.0355	0.0352	0.0348	0.0342	0.0333	0.0320	0.0303	0.0279	0.0242	0.0182

Table9 Stress intensity factor for a/b=1, ε=0.04

(a) Stress intensity factor F_I

ν_1	ν_2	μ_2/μ_1	0/11	1/11	2/11	3/11	4/11	5/11	6/11	7/11	8/11	9/11	10/11
0.3	0.3	2.5557	0.7509	0.7492	0.7440	0.7351	0.7219	0.7040	0.6804	0.6495	0.6080	0.5470	0.4377
0	0.5	0.1667	0.7508	0.7492	0.7440	0.7350	0.7219	0.7040	0.6804	0.6495	0.6081	0.5471	0.4378
0	0	1.6667	0.7511	0.7494	0.7442	0.7352	0.7220	0.7040	0.6804	0.6494	0.6079	0.5468	0.4376

(b) Stress intensity factor F_{II}

ν_1	ν_2	μ_2/μ_1	0/11	1/11	2/11	3/11	4/11	5/11	6/11	7/11	8/11	9/11	10/11
0.3	0.3	2.5557	0.0542	0.0540	0.0535	0.0527	0.0514	0.0497	0.0474	0.0443	0.0403	0.0348	0.0265
0	0.5	0.1667	0.0537	0.0535	0.0531	0.0523	0.0511	0.0495	0.0472	0.0442	0.0403	0.0353	0.0277
0	0	1.6667	0.0550	0.0548	0.0543	0.0533	0.0519	0.0501	0.0476	0.0444	0.0401	0.0339	0.0243

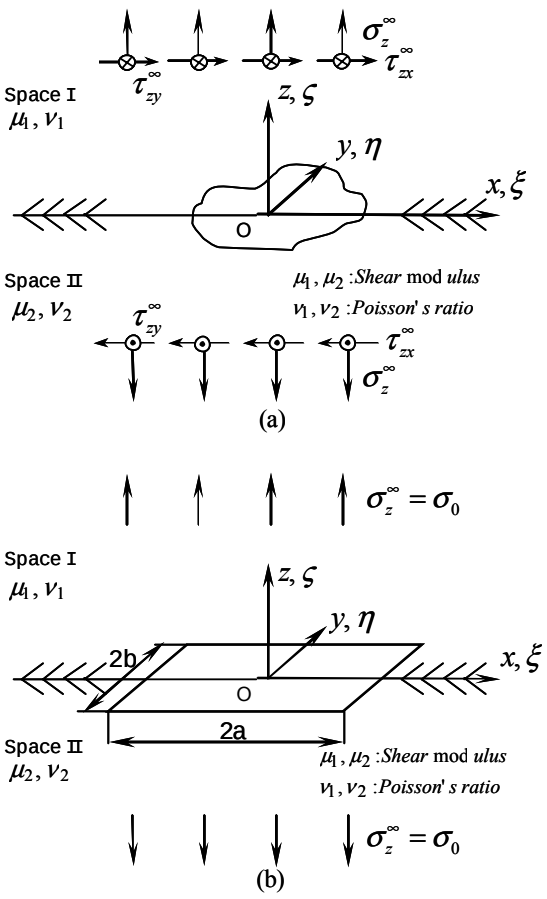

Fig.1 Problem configuration

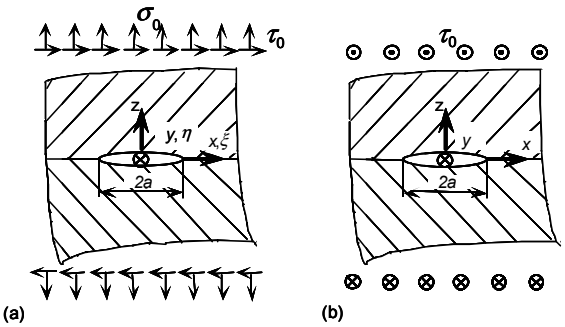

Fig2. Fundamental densities for two dimensional problems

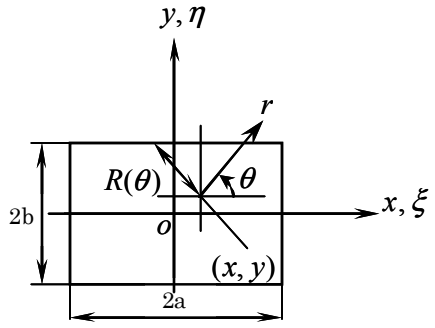

Fig.3 Integral parameters

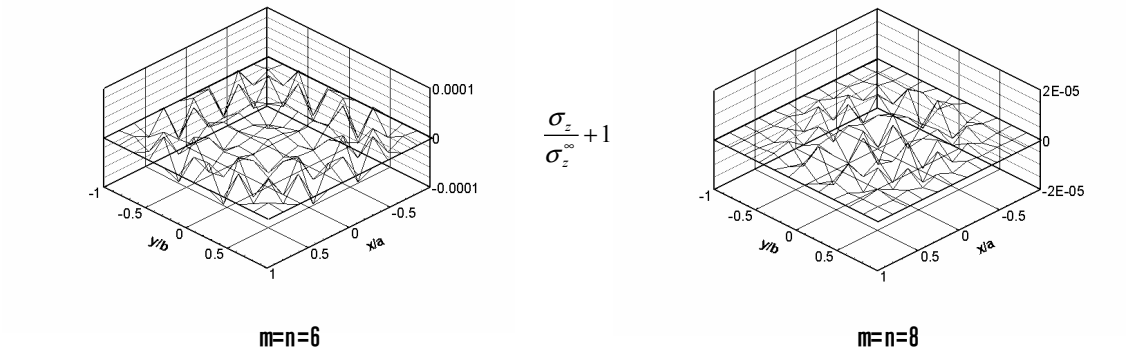

$\frac{\sigma_z}{\sigma_z^\infty}+1$

m=n=6 m=n=8

(a) $\frac{\sigma_z}{\sigma_z^\infty}+1\cong 0$

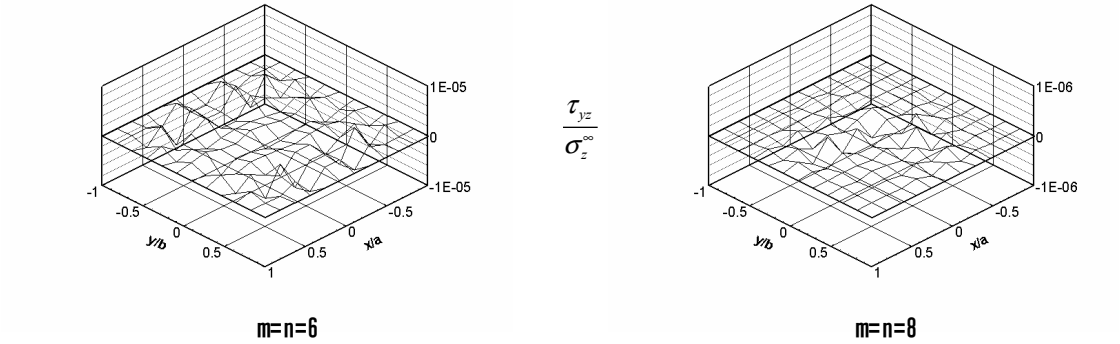

$\frac{\tau_{yz}}{\sigma_z^\infty}$

m=n=6 m=n=8

(b) $\frac{\tau_{yz}}{\sigma_z^\infty}\cong 0$

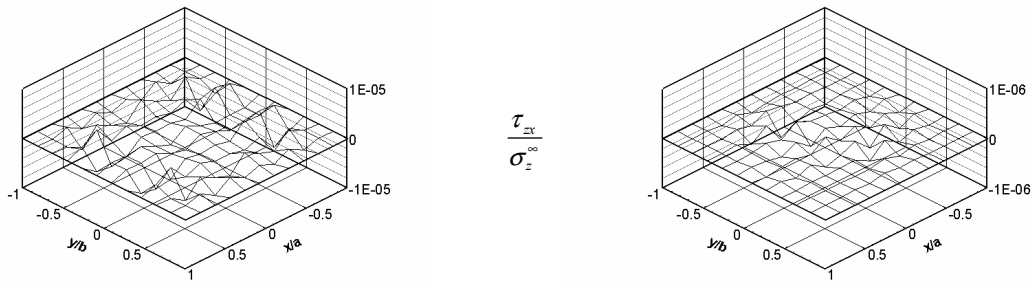

$\frac{\tau_{zx}}{\sigma_z^\infty}$

m=n=6 m=n=8

(c) $\frac{\tau_{zx}}{\sigma_z^\infty}\cong 0$

Fig.4 Compliance of boundary condition for $a/b=1, \varepsilon=0.02$